

Triplet Energy Migration in Poly(4-methacryloylbenzophenone-*co*-methyl methacrylate) Films: Temperature Dependence and Chromophore Concentration Dependence

Akira Tsuchida and Masahide Yamamoto*

Division of Polymer Chemistry, Graduate School of Engineering, Kyoto University, Yoshida, Sakyo-ku, Kyoto 606, Japan

William R. Liebe and Richard D. Burkhart

Department of Chemistry, University of Nevada, Reno, Nevada 89557-0020

Kyoji Tsubakiyama

Department of Applied Chemistry and Biotechnology, Faculty of Engineering, Fukui University, Bunkyo, Fukui 910, Japan

Received July 10, 1995; Revised Manuscript Received November 22, 1995*

ABSTRACT: Transient decays of triplet–triplet (TT) absorption of excited triplet benzophenone (BP) chromophore in poly(4-methacryloylbenzophenone-*co*-methyl methacrylate) (BPX, *X* is the mol % of BP, *X* = 1–100) films were studied by laser photolysis with a kinetic scheme involving a TT annihilation in a wide temperature range (20–240 K). The rate constant of the TT annihilation was analyzed by a diffusion model of the BP triplet state. The calculated diffusion coefficient (*D*) increased greatly with the increase of temperature and BP concentration in the BPX sample from $1 \times 10^{-11} \text{ cm}^2 \text{ s}^{-1}$ (20 K, *X* = 1) to $5 \times 10^{-7} \text{ cm}^2 \text{ s}^{-1}$ (240 K, *X* = 100). The steep increase in *D* was observed at the average BP distance less than 1.2 nm and above *ca.* 150 K. This temperature corresponds to *T_g* of poly(methyl methacrylate), α -methyl rotation.

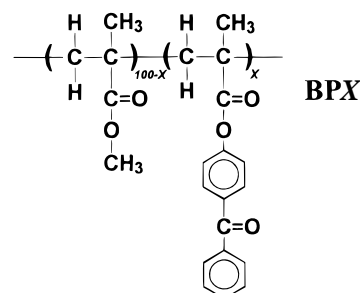
Introduction

Triplet energy migration and the subsequent triplet–triplet (TT) annihilation in polymer systems have been extensively studied through phosphorescence, delayed fluorescence, phosphorescence depolarization, and photochemical reactions.¹ Benzophenone (BP) is a chromophore suitable for the study of triplet energy migration and TT annihilation due to the high quantum efficiency of the intersystem crossing and the well-defined photophysical properties.^{2–5}

Guillet *et al.* reported that the phosphorescence emission intensity of a naphthalene chromophore does not change up to 230 K in poly(methyl methacrylate) (PMMA).^{1d} Horie *et al.* reported the intermolecular quenching of excited triplet BP (³BP*) doped in PMMA film by the carbonyl group of the PMMA side chain.⁶ The influence of this quenching on ³BP* phosphorescence decay was predominant at the temperature above *T_g* of PMMA (*ca.* 240 K, ester group rotation).⁶ On the other hand, when a fairly high intensity photoexcitation was applied to the sample, TT annihilation of ³BP* became major in comparison with other deactivation processes.³

In the present paper, the TT annihilation rate of the BP chromophore in poly(4-methacryloylbenzophenone-*co*-methyl methacrylate) (BPX, *X* is the mol % of BP unit) film was measured by the transient absorption of laser photolysis, and the rate was analyzed by a diffusion model of ³BP*. Polymer samples were prepared by a radical copolymerization of 4-methacryloylbenzophenone with methyl methacrylate, and then the aggregation-free homogeneous distribution of BP chromophore was achieved. The laser photolysis method has

an advantage that the concentration of ³BP* can be directly measured from the transient absorbance provided that the accurate molar extinction coefficient (ϵ) is available. The temperature of the sample films was changed over a wide range from 20 to 240 K *in vacuo*.



Experimental Section

Sample Preparation. 4-Methacryloylbenzophenone (MBP) monomer was synthesized from 4-hydroxybenzophenone (Tokyo Kasei Kogyo Co.) and methacryloyl chloride (Tokyo Kasei) by the similar method for 4-acryloylbenzophenone.⁷ Methacryloyl chloride (27 g, 0.26 mol) in dichloroethane (25 mL) was added dropwise under stirring to 4-hydroxybenzophenone (21 g, 0.11 mol) and pyridine (10 mL, 0.13 mol) dissolved in dichloroethane (750 mL). The reaction mixture was stirred for 3 h at room temperature. After the addition of 10 mL of methanol to stop the reaction, the reaction mixture was washed with water and then dried by anhydrous Na_2SO_4 . Solvent dichloroethane was removed by a rotary evaporator under reduced pressure. The crude product was purified by silica-gel column chromatography and eluted by toluene twice to give 12.0 g (0.045 mol, 43% yield) of pure MBP. *Mp*: 62–63 °C. ¹H NMR (CDCl_3): δ 2.08 (CH_3), 5.78 and 6.36 (CH_2), 7.18–7.92 (aromatic). IR (KBr): 3050, 2920, 1735, 1655, 1595, 1495, 1440, 1400, 1370, 1310, 1270, 1200, 1160, 1115, 1010, 935, 920, 880, 800, 780, 730, 690, 625, 495 cm^{-1} .

* Abstract published in *Advance ACS Abstracts*, February 1, 1996.

Table 1. Sample Characterization of BPX Polymers^a

polymer	$M_w/10^5$	$M_n/10^5$	M_w/M_n	film thickness/ μm	av BP separation/ b/nm
BP1	3.14	1.95	1.61	216	3.52
BP3	2.44	1.41	1.73	52.5	2.45
BP6	2.16	1.16	1.87	42.8	1.94
BP9	2.07	1.05	1.96	45.6	1.70
BP15	1.85	1.00	1.84	66.6	1.43
BP24	2.14	1.05	2.04	38.9	1.23
BP32	1.99	1.03	1.93	33.6	1.11
BP44	1.75	0.810	2.16	36.3	1.00
BP65	1.78	0.856	2.08	24.0	0.880
BP100	1.60	0.741	2.16	18.7	0.762

^a X of BPX denotes the mol % of BP unit in the copolymer.

^b Calculated by (volume/number of BP unit therein)^{1/3}.

Methyl methacrylate (MMA) monomer (Wako Pure Chemical Industries, Ltd.) was purified by the same procedure as already reported.⁸

Copolymers (BPX) of MBP with MMA were obtained by a radical copolymerization initiated by AIBN in degassed benzene at 60 °C.⁹ After the purification by repeated precipitations of a dichloromethane solution into methanol, molecular weights of BPX polymers were determined by GPC (Toyo Soda HLC 802UR, polystyrene standard), as shown in Table 1. The mol % of BP unit in BPX samples was determined by the UV absorbance of the BP band (338.5 nm peak) using BP100 (poly-(4-methacryloylbenzophenone) homopolymer) as a standard in dichloromethane solvent.

Sample films of BPX for measurements were prepared by the solution cast method on a quartz plate. 1,2-Dichloroethane (Dotite Spectrosol) solvent for the cast was removed from the film by evacuation in a desiccator. The film thickness shown in Table 1 was calculated from the polymer weight cast on a quartz plate assuming the polymer density 1.0 g cm⁻³.

Laser Photolysis. Transient absorption spectra and decays of BPX films were obtained by the laser photolysis system whose details have already been reported.¹⁰ Sample excitation was made by the 308-nm light (XeCl gas) pulse of a Questek Model 2110 excimer laser. The excitation pulse energy was appropriately attenuated by filters, and the regular photon energy per a pulse at the sample position was measured as 1.1 mJ cm⁻² by a power meter.

Transient absorption spectra were recorded by an optical multichannel analyzer (OMA) system composed of a Princeton Instruments IRY-700S/B detector, PG-10 pulse generator, ST-120 controller, and a polychromator (SPEX). Transient absorption decays were collected at 540 nm by an R928 photomultiplier (Hamamatsu) fitted with a monochromator and a digital oscilloscope (LeCroy 9410).¹¹ Water and band-pass filters were used for the probing light of a xenon lamp to avoid the short UV and heat irradiation of the samples.

The sample temperature was controlled by a closed cycle helium cryostat system (APD Cryogenics Inc.) in degassed conditions. Sample films cast on a quartz disk were mounted in a copper cryotip tightly by using indium gaskets.

Results and Discussion

Transient Absorption Spectra and Decays. Table 1 shows the characterization of 10 BPX polymer samples with the average separation distances of BP chromophores in the films. All cast films of BPX polymers were colorless and transparent in spite of a fairly large thickness, e.g., even the BP1 sample.

Figure 1 shows the transient absorption spectrum of BP3 film measured by OMA at 298 K *in vacuo*. The 540-nm absorption band in this figure was ascribed to ³BP* whose band position has been reported in many references.¹² Here we could not detect the ketyl radical which may be produced by the hydrogen abstraction of ³BP*. Melhuish has already reported the absence of the ketyl radical for BP-doped PMMA solid by flash photolysis measurements.^{12b} No noticeable peak shift of

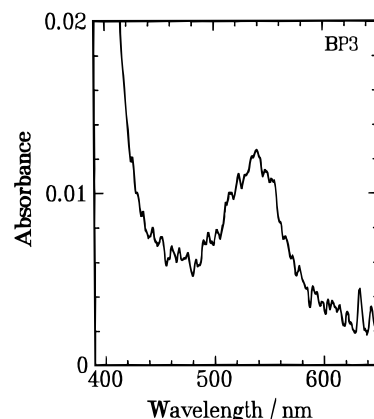


Figure 1. Transient absorption spectrum of the BP3 film measured by laser photolysis at 298 K *in vacuo*. Spectrum was obtained at 180 ns after excitation with a 140 ns gate width of an image intensifier.

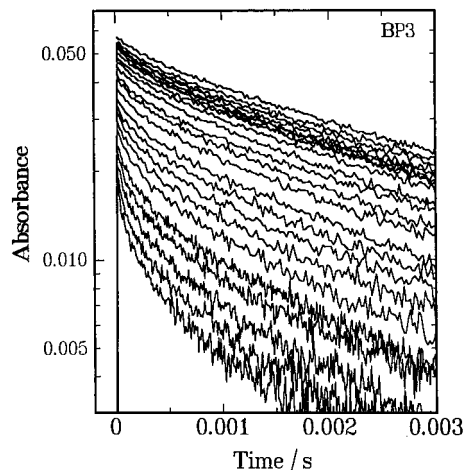


Figure 2. Transient absorption decays of the BP3 film measured by laser photolysis at 540 nm. Sample temperature was changed from 20 K (top) to 240 K (bottom) by every 10 K separation.

this band was observed by the change of temperature, the delay time of the image intensifier gate, and BP mol % in the range of the measurements.

Transient decays of the ³BP* absorption band peak at 540 nm were measured for BPX polymers in the temperature range 20–240 K. Guillet *et al.* reported that the phosphorescence intensity of a naphthalene chromophore does not change up to 230 K in PMMA in the absence of oxygen.^{1d} Horie *et al.* reported that the carbonyl group of the PMMA side chain quenches ³BP* intermolecularly;⁶ however, the degree of this kind of quenching is also negligible in the present temperature range.

Figure 2 shows the temperature effect on ³BP* decays for the BP3 film. The decay rate was accelerated with the increase of temperature from 20 to 240 K. Other polymers of BPX gave the same tendency, though the decay time scale was greatly reduced to submicrosecond order for the high BP loading polymers at high temperatures. The large temperature effect on the decay rates was observed for the large BP mol % polymers.

Figure 3 shows the ³BP* decays measured at 120 K for the BPX films with different BP mol %. This figure clearly indicates that the large BP loading gives the large decay rates of ³BP*. This result was the same for all other temperatures. David *et al.* reported the similar concentration effect of ³BP* for the copolymers of

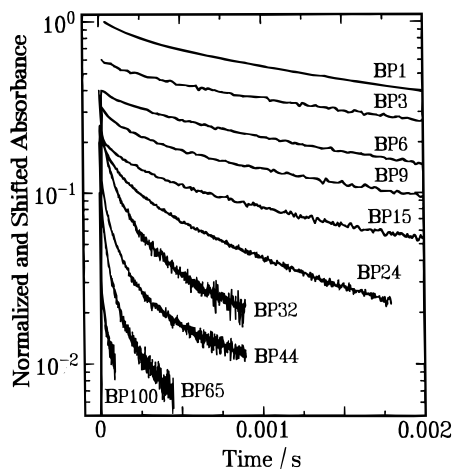


Figure 3. Transient absorption decays of the BPX films measured by laser photolysis at 120 K. Every decay was normalized by the peak absorbance and was shifted for display.

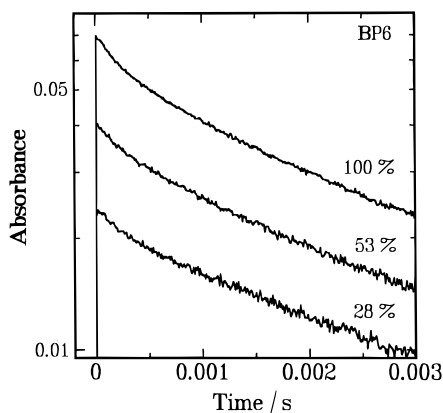


Figure 4. Transient absorption decays of the BP6 film measured by laser photolysis at 30 K. Excitation laser intensity was attenuated by filters; 100% (top), 53% (middle), and 28% (bottom).

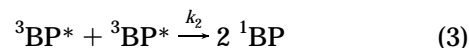
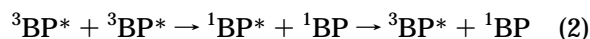
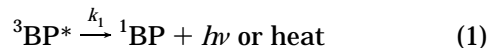
styrene-vinylbenzophenone by phosphorescence decay measurements.^{2c} The effect was attributed to the increase of triplet energy migration efficiency with the increase of BP content as the result of the large exchange interaction between BP groups. The increase of triplet energy migration rate among BP chromophores enhanced the TT annihilation of $^3\text{BP}^*$, resulting in the fast decay of $^3\text{BP}^*$.

In order to confirm the participation of the TT annihilation in the $^3\text{BP}^*$ decay for the present system, the excitation intensity effect was examined by changing the excitation laser intensity with filters. Figure 4 shows the $^3\text{BP}^*$ decays for BP6 copolymer with different excitation laser intensities of 100% (top), 53% (middle), and 28% (bottom), measured at 30 K. From the figure, one can see that the high excitation intensity induced a large bend of the decay in the initial time range of 0–1 ms. It is noticeable that, in spite of the different initial bend, the decay slopes in the long time scale (>2 ms) give almost the same decrease rate irrespective of the excitation intensity; approximately the same exponential decay rate was observed further in the long time scale. TT annihilation of $^3\text{BP}^*$ is a bimolecular process caused by the interaction of two $^3\text{BP}^*$ transient intermediates. Therefore, the high $^3\text{BP}^*$ concentration immediately after the pulse photoexcitation induces the nonexponential decay. However, the contribution of the TT annihilation comes to be minor in the long time scale, where the concentration of $^3\text{BP}^*$ is low and the

decay exhibits the intrinsic deactivation rate of the $^3\text{BP}^*$ at the temperature.

Decay Analysis. The decay rate of $^3\text{BP}^*$ in the BPX films was greatly affected by the change of temperature and BP mol %, as mentioned above. The transient decays measured by laser photolysis were analyzed as follows.

The deactivation of $^3\text{BP}^*$ in the BPX films is represented by the following processes:



Equation 1 represents the intrinsic unimolecular deactivation of $^3\text{BP}^*$ to the ground state (^1BP), whose first-order rate constant is k_1 . Equations 2 and 3 are the TT annihilation process. If the repopulation process from $^3\text{BP}^*$ in eq 2 is neglected according to El-Sayed *et al.*,³ eq 4 is given, where k_2 is the second-order rate constant of eq 3.

$$-d[^3\text{BP}^*]/dt = k_1[^3\text{BP}^*] + 2k_2[^3\text{BP}^*]^2 \quad (4)$$

This rate constant of k_2 is now represented by the diffusion model proposed by Voltz *et al.* as follows:^{1,2,6,13,14}

$$k_2 = 4\pi RDN(1 + R/(\pi D t)^{1/2}) = A + B/t^{1/2} \quad (5)$$

with

$$A = 4\pi RDN$$

$$B = 4R^2(\pi D)^{1/2}N$$

where R is the reaction radius of TT annihilation between two $^3\text{BP}^*$, D is the sum of the diffusion coefficients from two $^3\text{BP}^*$, and N is the Avogadro number divided by 10^3 . Substituting eq 5 into eq 4, we get

$$-d[^3\text{BP}^*]/dt = k_1[^3\text{BP}^*] + 2(A + B/t^{1/2})[^3\text{BP}^*]^2 \quad (6)$$

Integration of eq 6 gives

$$[^3\text{BP}^*] = \frac{k_1}{-2A + \{Ck_1 + 2B(\pi k_1)^{1/2} \text{erf}((k_1 t)^{1/2})\}} \exp(k_1 t) \quad (7)$$

with C as a constant

$$C = 1/[^3\text{BP}^*]_0 + 2A/k_1$$

where $[^3\text{BP}^*]_0$ is the initial concentration of $^3\text{BP}^*$.

The value of k_1 is considered to be dependent on the temperature. The contribution of this k_1 to the $^3\text{BP}^*$ decay is predominant for the low BP loading BPX samples at low temperature, where the participation of TT annihilation is minor. Therefore, the value of k_1 was estimated from the long decay tail of the BP1 sample. Figure 5 shows the temperature dependence of the k_1 obtained; the values were almost the same for the 20–120 K region, whereas they increased above *ca.* 120 K. The broken line in the figure shows the average of the experimental points; k_1 taken from this line was used

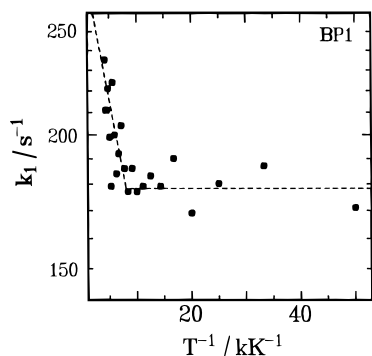


Figure 5. Plots of k_1 values vs T^{-1} for the BP1 sample. The broken line shows the temperature change of k_1 used for the decay fitting.

for the following decay fitting, and the values are given in Table 2. The values of k_1 in the table agreed fairly well with those obtained for BP6 in the long time range, irrespective of the different excitation intensities, as mentioned above.

The measured decay of $^3\text{BP}^*$ was fitted with eq 7 by the least-squares method of a Marquardt–Levenberg algorithm (Jandel, PeakFit). The molar extinction coefficient of $\epsilon = 4200 \text{ mol}^{-1} \text{ L cm}^{-1}$ was used for the TT absorption of $^3\text{BP}^*$ at 540 nm in order to convert the absorbance to $^3\text{BP}^*$ concentration.^{12b} The decay fitting by the free change of D , R , and $[^3\text{BP}^*]_0$ as the parameters was not successful; the value of R varied irregularly with the change of temperatures and BPX samples. Therefore, R was fixed tentatively at 1.5 nm^{-1} and D and $[^3\text{BP}^*]_0$ were changed as fitting parameters.

Figure 6 shows two examples of decay fitting with the best (upper) and the worst (lower) residuals. In Figure 6a, the calculated curve from the best-fit parameters cannot be seen due to the overlap with the dots of the experimental data. The absorbance decay shown in Figure 6b was measured in the short time range of submicroseconds. In this time range, the laser electromagnetic noise disturbed the photomultiplier signal. The D values obtained by the fitting are tabulated in Table 2. Larger D values were obtained at higher temperatures and higher BP mol % of BPX samples.

Figure 7 shows the temperature effect on D for the 10 BPX samples. At the low temperature range of 20–100 K, D was low and almost the same for all BP mol % samples. Then D gradually increased with the rise of temperature at 100–150 K, and finally, it steeply increased at $ca. >150 \text{ K}$. Up to now the temperature dependence of triplet state properties in polymer systems has been studied extensively by phosphorescence decay, intensity, and depolarization.^{1,2,4,6,15–17} In most of these reports, the discontinuity in the slope of Arrhenius plots was observed at the transition temperatures of the polymers investigated. PMMA has the transition temperature T_g at $ca. 150 \text{ K}$, which represents the onset of the α -methyl rotation of the chain.^{1,6,15–17} Then, the results shown in Figure 7 are interpreted by the increase of $^3\text{BP}^*$ migration rate above T_g . The coupling of the α -methyl rotation with the main chain induces the oscillation of the main chain,¹⁸ resulting in the fluctuation of BP chromophores, and the direct interaction of the α -methyl rotation with the chromophores also makes the chromophores fluctuate. The triplet exciton transfer depends critically on the distance between the donor and the acceptor. Then, the increase of chromophore fluctuation with temperature increases the probability for the chromophores to be

close enough for exciton transfer. The activation energies obtained at around 150–240 K in the figure for the BPX samples were $1.7\text{--}2.0 \text{ kcal mol}^{-1}$, which are close to those in references for the α -methyl group rotation.^{16,17}

Figure 8 shows the average BP distance dependence on D obtained at 20 and 240 K. At 20 K, $^3\text{BP}^*$ migration was not efficient for all the BPX samples, whereas at 240 K, D was greatly increased for the samples above 32 mol % of BP loading. This means that the $^3\text{BP}^*$ migration rate begins to increase at the BP chromophore average distance of less than $ca. 1.2 \text{ nm}$.

According to the three-dimensional random flight equation,

$$n = 6D/l^2 \quad (8)$$

where n is the hop frequency (the number of hops per second) of $^3\text{BP}^*$, D is the diffusion coefficient, and l is the interchromophore distance, which may be replaced by the average chromophore distance, as shown in Table 1. At present, an electron exchange Dexter mechanism is mostly accepted for triplet energy transfer.¹⁹ For the Dexter mechanism,

$$n(l) = (1/\tau_0) \exp[2(R_0 - l)/L] \quad (9)$$

where τ_0 is the lifetime of the excited state, R_0 is an interchromophore distance such that the probability of relaxation to the ground state is the same as that of energy transfer, and L is a constant called the "effective average Bohr radius".²⁰ According to eq 9, $\ln(n)$ vs l should be a straight line.

Figure 9 shows the average chromophore distance (l) dependence of $\ln(n)$ which was calculated by D in Table 2. As shown in the figure, however, it was difficult to find a linear relation between $\ln(n)$ and l for the whole range of l from BP1 through BP100. At 240 K in the short l region, where the energy migration is efficient and averaged enough, one could argue that the five experimental points for BP24 through BP100 obey the Dexter equation. A least-squares line for the five points as shown in the figure by (a) yielded $R_0 = 2.3 \text{ nm}$ and $L = 0.20 \text{ nm}$, whose values are of acceptable order though a little larger than those already reported.^{1,20} However at 20 K, a least-squares line for the five experimental points for BP24 through BP100, as shown by line b, yielded $R_0 = 3.7 \text{ nm}$ and $L = 0.90 \text{ nm}$, whose values are too large to accept. David *et al.* measured the triplet energy migration in copolymers of styrene–vinylbenzophenone at 77 K.^{2c} They reported that their results are in agreement with Voltz's theory at moderate vinylbenzophenone content ($<50 \text{ mol } \%$). In the present study of a wide temperature range from 20 to 240 K, however, it was difficult to obtain a unique pair of R_0 and L . This result may be interpreted by assuming that (i) migration will occur to the nearest neighbor and the nearest neighbor distance may well be smaller than the average chromophore distance calculated by the chromophore concentration and/or (ii) trap concentration and energy may be dependent on temperature and time.

Validity of the Estimation. The definition of the D value obtained in this work is the sum of the diffusion coefficients of two $^3\text{BP}^*$. Therefore half of the D corresponds to the diffusion coefficient for single $^3\text{BP}^*$. Similar order D values have been reported by David *et al.* for vinylbenzophenone copolymers at 77 K.^{2c}

Table 2. Values of D Obtained by the Curve Fitting

temp/K	k_1/s^{-1}	$D/10^{-10} \text{ cm}^2 \text{ s}^{-1}$									
		BP1	BP3	BP6	BP9	BP15	BP24	BP32	BP44	BP65	BP100
20	178	0.119	0.333	0.203	0.670	0.490	0.489	3.29	1.85	1.02	0.971
30	178	0.126	0.332	0.239	0.593	0.596	0.609	4.99	2.11	1.32	1.07
40	178	0.121	0.291	0.230	1.00	0.299	0.481	6.56	2.35	1.54	1.53
50	178	0.128	0.185	0.220	0.911	0.448	0.711	4.53	1.93	1.94	1.84
60	178	0.173	0.208	0.261	0.953	0.434	1.03	6.98	3.47	2.24	3.77
70	178	0.195	0.228	0.263	1.07	0.568	1.32	10.9	5.19	4.03	6.95
80	178	0.246	0.272	0.235	1.01	0.692	1.61	17.6	7.71	7.99	13.5
90	178	0.297	0.282	0.363	1.36	0.844	2.59	25.1	13.3	14.8	27.9
100	178	0.350	0.344	0.370	1.34	1.00	3.37	31.6	20.7	27.1	86.4
110	178	0.463	0.464	0.420	1.23	1.30	2.10	47.4	37.7	57.5	176
120	178	0.515	0.437	0.494	1.36	1.39	3.15	64.8	56.6	98.8	265
130	185	0.719	0.627	0.584	1.22	2.22	4.70	97.9	93.1	173	393
140	191	0.811	0.617	0.633	1.85	2.46	6.18	123	203	299	594
150	195	1.50	0.937	0.698	2.21	3.32	9.61	161	204	482	765
160	201	1.30	0.999	0.834	2.44	4.88	13.1	248	280	727	1080
170	206	1.60	1.17	1.03	2.98	6.61	16.4	333	365	1040	1480
180	208	2.19	1.55	1.18	3.73	8.90	20.4	403	488	1320	1990
190	213	2.89	2.17	1.62	4.31	13.3	27.3	524	646	1670	2500
200	216	3.59	3.17	1.89	4.55	18.1	33.8	685	913	2150	2750
210	219	6.03	3.78	2.84	5.34	26.8	43.9	966	1230	2710	3330
220	220	7.06	5.85	3.70	5.87	34.3	54.2	1210	1460	3150	3780
230	225	9.64	7.67	4.79	8.09	47.6	73.0	1250	1720	3830	4530
240	232	9.88	10.1	7.97	9.54	69.8	90.2	1670	2110	4430	5140

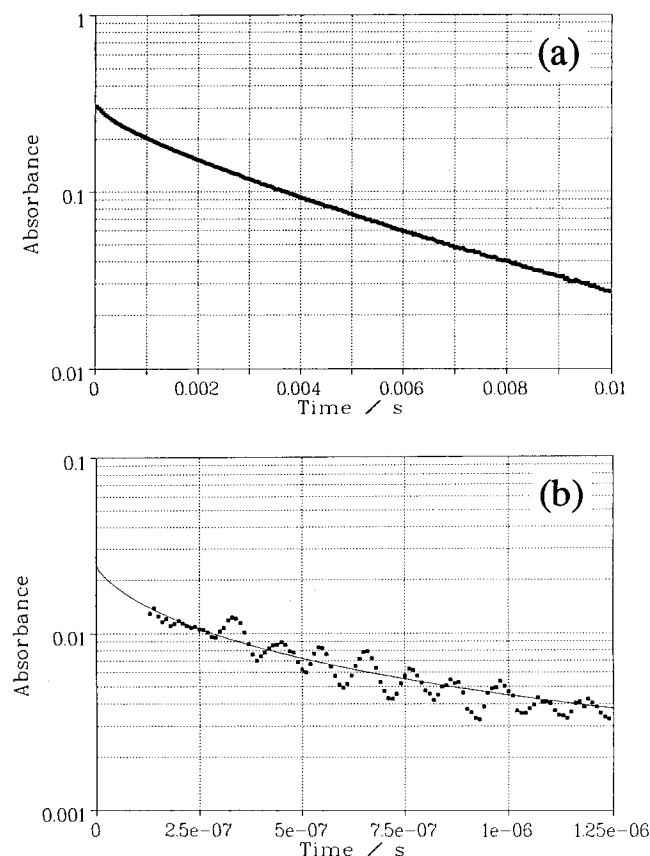


Figure 6. Examples of the decay fitting. (a) The most successful fitting for the BP1 sample at 60 K. The calculated curve from the best-fit parameters ($D = 1.73 \times 10^{-11} \text{ cm}^2 \text{ s}^{-1}$, $[^3\text{BP}^*]_0 = 3.47 \times 10^{-3} \text{ mol L}^{-1}$) cannot be seen due to the overlap with the measured decay (square dots). (b) The most poor fitting for the BP100 sample at 240 K. The center fine line shows the calculated curve from the best-fit parameters ($D = 5.14 \times 10^{-7} \text{ cm}^2 \text{ s}^{-1}$, $[^3\text{BP}^*]_0 = 3.18 \times 10^{-3} \text{ mol L}^{-1}$) of the measured decay (square dots).

Next, discussion will be given on how the estimation error of parameters affects the results of decay fitting, taking the value of $D = 1.19 \times 10^{-11} \text{ cm}^2 \text{ s}^{-1}$ obtained for the BP1 sample at 20 K as an example.

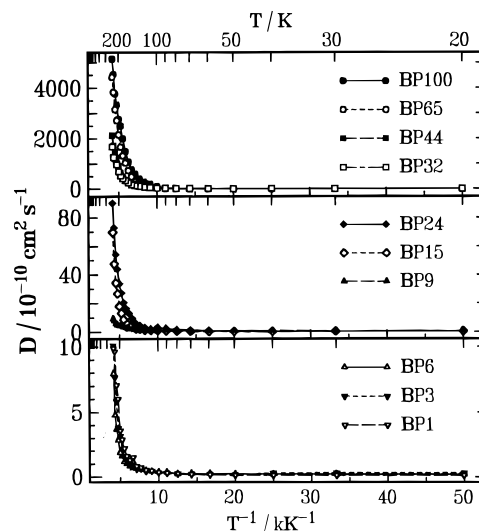


Figure 7. Plots of D values vs T^{-1} for the BPX samples. Exact values are given in Table 2.

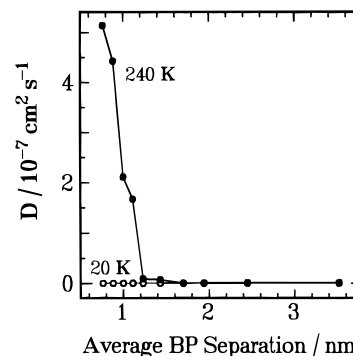


Figure 8. Plots of D values vs the average BP distance at 20 K (open circles) and 240 K (closed circles).

(1) The molar extinction coefficient (ϵ) of $^3\text{BP}^*$ may be changed by the medium used. We adopted the value of $\epsilon = 4200 \text{ mol}^{-1} \text{ L cm}^{-1}$ obtained in PMMA solid.^{12b} The values measured in solution in recent years are rather high, such as $\epsilon = 6500 \text{ mol}^{-1} \text{ L cm}^{-1}$.^{12a,c,d} If this ϵ is used for the fitting, $D = 2.03 \times 10^{-11} \text{ cm}^2 \text{ s}^{-1}$ is calculated.

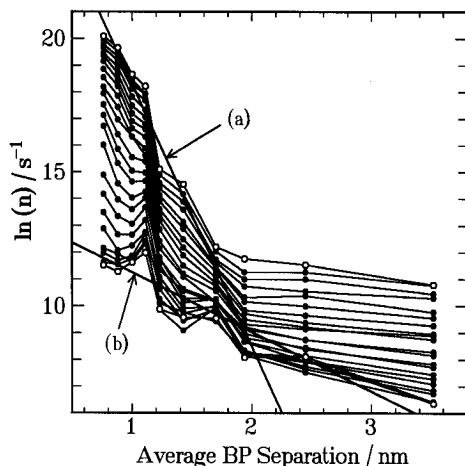


Figure 9. Plots of $\ln(n)$ values vs the average BP separation as shown in Table 1. The temperature was changed from 20 K (bottom) to 240 K (top). The straight lines of (a) and (b) show the least-squares lines calculated from the five experimental points of BP24 through BP100 at 240 K (a) and 20 K (b), respectively (open circles).

(2) A reaction radius of $R = 1.5$ nm was assumed for the fitting. If we use $R = 1.0$ and 2.0 nm, then $D = 2.24 \times 10^{-11}$ and 6.91×10^{-12} $\text{cm}^2 \text{s}^{-1}$ are given, respectively.

(3) The estimation error of k_1 also affects the fitting results. If we use $k_1 = 196 \text{ s}^{-1}$ (+10%) and 160 s^{-1} (−10%), then $D = 8.58 \times 10^{-12}$ and 1.55×10^{-11} $\text{cm}^2 \text{s}^{-1}$ are obtained as the best fittings, respectively. However, the contribution of k_1 to the decay was minor for high BP mol % samples in the high-temperature region.

(4) The most unlikely assumption of the present analysis is the neglect of eq 2, which is the repopulation process of $^3\text{BP}^*$ by TT annihilation. On the other hand, as another extreme case, if we neglect eq 3 instead of eq 2, then eq 6 changes to

$$-d[^3\text{BP}^*]/dt = k_1[^3\text{BP}^*] + (a + b/t^{1/2})[^3\text{BP}^*]^2 \quad (10)$$

with

$$a = 4\pi rdN$$

$$b = 4r^2(\pi D)^{1/2}N$$

where r and d are the new R and D , respectively. These substitutions of $2A = a$ and $2B = b$ finally result in $r = 2^{1/3}R$ and $d = 2^{2/3}D$. In other words, the same fitting can be obtained by using a new pair of r and d . This will only affect the calculated value of the diffusion coefficient. For the more serious case, if the contribution ratio of eq 2 to eq 3 for the consumption of $^3\text{BP}^*$ is temperature-dependent, a maximum estimation error by a factor of $2^{1/3}$ and $2^{2/3}$ may be added to r and d , respectively.

Conclusions

$^3\text{BP}^*$ decays in the BPX films were analyzed by a kinetic scheme involving a TT annihilation process at 20–240 K. The temperature dependence and BP concentration dependence of the diffusion coefficient of $^3\text{BP}^*$ in the films were shown by the use of a diffusion model under the assumption of $R = 1.5$ nm and $\epsilon(^3\text{BP}^* \text{ at } 540 \text{ nm}) = 4200 \text{ mol}^{-1} \text{ L cm}^{-1}$. The obtained value of D increased with the increase of temperature and with the increase of BP mol % in the BPX samples. The steep

increase in D was observed at the temperature above 150 K (T_g) and at the average BP separation distance of <1.2 nm.

Acknowledgment. We are indebted to Professors K. Razi Naqvi (University of Trondheim) and J. Fredrick (University of Nevada, Reno) for their helpful comments. This work was supported by the Japan-U.S. Cooperative Science Program of Japan Society for the Promotion of Science (JSPS) and by the NSF U.S.-Japan Cooperative Research Program. The authors at Nevada acknowledge support by the U.S. Department of Energy under Grant No. DE-FG03-92ER45476.

References and Notes

- (1) (a) Birks, J. B. *Photophysics of Aromatic Molecules*; Wiley Interscience: New York, 1970. (b) Turro, N. J. *Modern Molecular Photochemistry*; Benjamin Cummings: Menlo Park, CA, 1978. (c) Semerak, S.; Frank, C. W. *Adv. Polym. Sci.* **1983**, *54*, 31. (d) Guillet, J. *Polymer Photophysics and Photochemistry*; Cambridge University Press: London, 1985. (e) *Polymer Photophysics*; Phillips, D., Ed.; Chapman and Hall: London, 1985. (f) *Photophysical and Photochemical Tool in Polymer Science*; Winnik, M. A., Ed.; Reidel: Dordrecht, 1986. (g) Ushiki, H.; Horie, K. *Handbook of Polymer Science and Technology*; Cheremisinoff, N. P., Ed.; Marcel Dekker: New York, 1989; Vol. 4. References cited in these reviews are also relevant.
- (2) (a) David, C.; Demarteau, W.; Geuskens, G. *Eur. Polym. J.* **1970**, *6*, 537. (b) David, C.; Baeyens-Volant, D.; Geuskens, G. *Eur. Polym. J.* **1976**, *12*, 71. (c) David, C.; Baeyens-Volant, D.; Macedo de Abreu, P.; Geuskens, G. *Eur. Polym. J.* **1977**, *13*, 841.
- (3) (a) El-Sayed, F. E.; MacCallum, J. R.; Pomery, P. J.; Shepherd, T. M. *J. Chem. Soc., Faraday Trans. 2* **1979**, *75*, 79. (b) Jassim, A. N.; MacCallum, J. R.; Moran, K. T. *Eur. Polym. J.* **1983**, *19*, 909. (c) Fraser, I. M.; MacCallum, J. R.; Moran, K. T. *Eur. Polym. J.* **1984**, *20*, 425.
- (4) Haggquist, G. W.; Burkhart, R. D. *Chem. Phys. Lett.* **1988**, *152*, 56.
- (5) (a) Schnabel, W. *Macromol. Chem.* **1979**, *180*, 1487. (b) Salmassi, A.; Schnabel, W. *Polym. Photochem.* **1984**, *5*, 215.
- (6) (a) Horie, K.; Mita, I. *Chem. Phys. Lett.* **1982**, *93*, 61. (b) Horie, K.; Morishita, K.; Mita, I. *Macromolecules* **1984**, *17*, 1746. (c) Horie, K.; Mita, I. *Eur. Polym. J.* **1984**, *20*, 1037.
- (7) Carlini, C.; Ciardelli, F.; Donati, D.; Gurzoni, F. *Polymer* **1983**, *24*, 599.
- (8) Tsuchida, A.; Sakai, W.; Nakano, M.; Yamamoto, M. *J. Phys. Chem.* **1992**, *96*, 8855.
- (9) Tsujii, Y.; Tsuchida, A.; Onogi, Y.; Yamamoto, M. *Macromolecules* **1990**, *23*, 4019.
- (10) Ganguly, T.; Burkhart, R. D.; Nelson, J. H. *J. Phys. Chem.* **1994**, *98*, 5670.
- (11) Razi Naqvi, K.; Haggquist, G. W.; Burkhart, R. D.; Sharma, D. K. *Rev. Sci. Instrum.* **1992**, *63*, 5806.
- (12) (a) Carmichael, I.; Hug, G. L. *J. Phys. Chem. Ref. Data* **1986**, *15*, 54. (b) Melhuish, W. H. *Trans. Faraday Soc.* **1966**, *62*, 3384. (c) Bensasson, R. V.; Gramain, J.-C. *J. Chem. Soc., Faraday Trans. 1* **1980**, *76*, 1801. (d) Baral-Tosh, S.; Chattopadhyay, S. K.; Das, P. K. *J. Phys. Chem.* **1984**, *88*, 1404.
- (13) Voltz, R.; Laustriat, G.; Coche, A. *J. Chim. Phys.* **1966**, *63*, 1253.
- (14) North, A. M.; Treadaway, M. F. *Eur. Polym. J.* **1973**, *9*, 609.
- (15) Graves, W. E.; Hofeldt, R. H.; McGlynn, S. P. *J. Chem. Phys.* **1972**, *56*, 1309.
- (16) Somersall, A. C.; Dan, E.; Guillet, J. E. *Macromolecules* **1974**, *7*, 233.
- (17) Rutherford, H.; Soutar, I. *J. Polym. Sci., Polym. Phys. Ed.* **1980**, *18*, 1021.
- (18) Tanabe, Y.; Hirose, J.; Okano, K.; Wada, Y. *Polym. J.* **1970**, *1*, 107.
- (19) Dexter, D. L. *J. Chem. Phys.* **1953**, *21*, 836.
- (20) Inokuti, M.; Hirayama, F. *J. Chem. Phys.* **1965**, *43*, 1978.

MA9509671